Vol 12 No 10, October 2003
1009-1963/2003/12(10)/1124-11

Chinese Physics

© 2003 Chin. Phys. Soc.
and IOP Publishing Ltd

Self-deflection of a bright soliton in a separate bright–dark spatial soliton pair based on a higher-order space charge field*

Liu Jin-Song(刘劲松)† and Hao Zhong-Hua(郝中华)‡

State Key Laboratory of Laser Technology, Huazhong University of Science and Technology, Wuhan 430074, China

(Received 3 January 2003; revised manuscript received 20 May 2003)

The self-deflection of a bright solitary beam can be controlled by a dark solitary beam via a parametric coupling effect between the bright and dark solitary beams in a separate bright–dark spatial soliton pair supported by an unbiased series photorefractive crystal circuit. The spatial shift of the bright solitary beam centre as a function of the input intensity of the dark solitary beam ($\hat{\rho}$) is investigated by taking into account the higher-order space charge field in the dynamics of the bright solitary beam via both numerical and perturbation methods under steady-state conditions. The deflection amount (Δs_0), defined as the value of the spatial shift at the output surface of the crystal, is a monotonic and nonlinear function of $\hat{\rho}$. When $\hat{\rho}$ is weak or strong enough, Δs_0 is, in fact, unchanged with $\hat{\rho}$, whereas Δs_0 increases or decreases monotonically with $\hat{\rho}$ in a middle range of $\hat{\rho}$. The corresponding variation range (δs) depends strongly on the value of the input intensity of the bright solitary beam (r). There are some peak and valley values in the curve of δs versus r under some conditions. When $\hat{\rho}$ increases, the bright solitary beam can scan toward both the direction same as and opposite to the crystal's c-axis. Whether the direction is the same as or opposite to the c-axis depends on the parameter values and configuration of the crystal circuit, as well as the value of r. Some potential applications are discussed.

Keywords: spatial optical solitons, photorefractive effects, photovoltaic effects, self-deflection
PACC: 4265J, 4265S

1. Introduction

Optical spatial solitons have been extensively studied during the last three decades.[1] To date, many topics have been researched in the areas including Kerr solitons, photorefractive (PR) solitons, incoherent solitons, quadratic solitons, Bragg solitons, discrete solitons, cavity solitons and magneto-optic solitons, and so on.[2] PR spatial solitons have become a convenient playground to study soliton phenomena, since they are observed at low light powers and exhibit robust trapping in both transverse dimensions; and, at present, the investigations on the PR solitons, soliton pair and soliton interaction are concerned with a single PR crystal.[3−19] Very recently, we have suggested a crystal circuit in which two PR crystals, at least one being photovoltaic-photorefractive (PV-PR), link up in a chain by electrode leads with or without a voltage source, and we predict that each crystal could support a steady-state one-dimensional bright or dark spatial soliton.[20−22] The two solitons, formed separately in the two crystals, were named a separate spatial soliton pair. Both bright and dark steady-state PR solitons, including screening solitons,[4] closed-circuit photovoltaic solitons[5] and screening-photovoltaic (SP) solitons,[6] could form in the crystals. As a result, there are three possible realizations of the separate spatial soliton pairs: bright–bright, bright–dark and dark–dark. For the solitons supported by such a crystal circuit, although the conditions for the existence of a soliton in each crystal are not new, i.e., the conditions are same as that for a single PR crystal, it is new that the two solitons, supported separately by two crystals, could affect each other since the linked crystals could create a parametric coupling that results from the parametric depen-

*Project supported by the National Natural Science Foundation of China (Grant No 10174025) and the Key Project Foundation of the Education Ministry of China (Grant No 01118).

†E-mail: jsliu4508@vip.sina.com
‡Present address: Institute of Applied Physics, Xidian University, Xi'an 710071, China.

dence on the dynamics when initial conditions change. Such a parametric, other than dynamic, coupling effect not only could affect the characters of the two solitons in a pair, including the spatial profiles, dynamical evolutions, stabilities and self-deflections, but also could bring about some new phenomena that never occurred for those solitons or soliton pairs supported by a single PR crystal. The coupling effects between the two solitons in a pair on the intensity profiles, dynamical evolutions, stabilities and self-deflection of the two solitons have been investigated numerically and in detail on biased[20] and unbiased[22] PR circuits, and many new phenomena also have been revealed, in which the most interesting one is that the dark soliton could affect the bright one by light-induced current, whereas the bright soliton could not affect the dark one in a bright–dark soliton pair in the limit that the optical wave is in a spatial extent much less than the width of the crystal. This unilateral effect may be useful in some applications, such as unidirectional optical couplers, new optical switching technology and novel optical deflectors.

PR solitons are promising in the application of making an optically controlled optical deflector or scanner due to their self-deflection, which can be adjusted by another light beam. The self-deflection of PR solitons in a biased PR crystal has been lucubrated by many researchers experimentally and theoretically.[23–29] The stronger the biased field, the larger the deflection range of a PR bright soliton is, since the higher-order space charge fields can enhance the process of the self-deflection when the biased field is strong enough.[26,27] If a light beam is incident upon a biased PR crystal in which a PR bright soliton has formed, then variation of the input intensity of the light beam will lead to variation in the background light of the crystal, thereby changing the self-deflection of the bright soliton. That is, varying the input intensity of the light beam can control the self-deflection of the bright soliton. Obviously, it is beneficial to providing a strong biased field. However, the stronger the biased field, the more difficult the application of it to the crystal. Fortunately, this difficulty can be overcome by use of an unbiased series PR crystal circuit. Let a separate bright–dark soliton pair form in the circuit, then the self-deflection of the bright soliton can be controlled by the dark soliton without a biased field. Of course, it is beneficial to use a PV-PR crystal with a strong photovoltaic field.

In this paper, we investigate how to use the dark soliton to control the self-deflection of the bright soliton in a separate bright–dark soliton pair supported by an unbiased series PR crystal circuit in which the crystals possess a strong photovoltaic field. Obviously, the effects of the higher-order space charge field on the self-deflection of a bright soliton should be considered. Our results show that varying the input intensity of the dark soliton can effectively control the amount of deflection and the direction of the bright soliton.

This paper is organized as follows. In Section 2, we expand our previous work[21] to include the diffusion term and the higher-order space charge fields in the theoretical model for a bright soliton. A system of two coupled dynamical evolution equations is derived for a bright–dark soliton pair, in which the first-order diffusion term and the higher-order odd perturbation terms resulting from the higher-order space charge fields are included in the equation of the bright soliton. In Section 3, some numerical results are obtained for the dynamical self-deflection evolution of the bright soliton with different values of the input intensity of the dark soliton. In Section 4, these problems are further studied using perturbation procedures. Some analytical formulae to describe the self-deflection of the bright soliton are then derived. A lot of general information is obtained from these analytical analyses. The analytical results are compared with those obtained numerically and are found to be in good agreement. Finally, we summarize the results, discuss their significance in the application of an optical beam deflector or scanner and draw some conclusions in Section 5.

2. Theoretical model

Figure 1 shows an unbiased series PR crystal circuit in which two crystals, denoted by P and $\hat{P}$, at least one being PV-PR, are connected electronically in a chain by electrode leads. For each crystal, electrodes are made on the two surfaces with their normal parallel to the c-axis of the crystal. In the limit that the optical wave has a spatial extent Δx much less than the x width of the crystal (the x-direction being taken parallel to the c-axis), we have predicted that each crystal could support a spatial bright (dark) soliton.[21] We named the two solitons, supported separately by the two crystals, a separate spatial soliton pair.

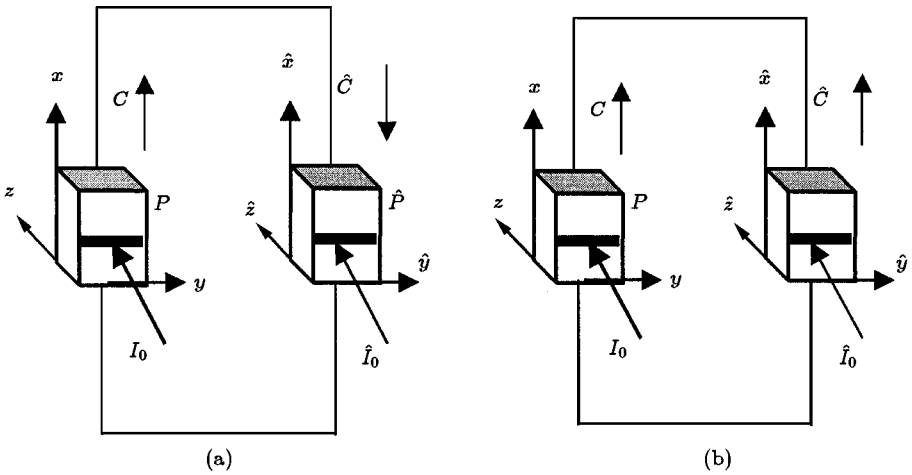


Fig.1. Illustration of the series PR crystal circuit consisting of two PR crystals in which at least one crystal must be PV-PR. (a) The two crystals' c-axes are oriented in the left-handed screw sense, denoted by $\uparrow\uparrow$, and (b) one crystal's c-axis is oriented in the right-handed screw sense but the other crystal's c-axis is oriented in the left-handed screw sense, denoted by $\uparrow\downarrow$. P and $\hat{P}$ denote the two crystals respectively. C and $\hat{C}$ denote the two c-axes. I_0 and $\hat{I}_0$ denote the incident bright or dark soliton-like one-dimensional laser beams.

There are three possible realizations of the separate spatial soliton pairs: bright–bright, bright–dark and dark–dark. In this paper, we only consider the bright–dark soliton pairs. We assume that the bright soliton forms in the crystal P and the dark one forms in the crystal $\hat{P}$. Each crystal is oriented with its c-axis perpendicular to the direction of the laser beam, which is polarized parallel to the c-axis. The optical beam propagates in the crystal along the z-direction and is permitted to diffract only along the x-direction. The theoretical model about the separate spatial soliton pairs formed in such a circuit was built in Ref.[21] in which the diffusion process and the higher-order space charge fields were not considered. In order to expand the theoretical model to include the diffusion process and the higher-order space charge field, at first, we make a brief introduction of the results obtained in Ref.[21] only for a bright–dark soliton pair as follows.

The expressions of induced space charge field $E_{\rm sc}$ in the crystal P and $\hat{E}_{\rm sc}$ in the crystal $\hat{P}$ are

$$E_{\rm sc} = E_0 \frac{I_{\rm d}}{I + I_{\rm d}} - E_{\rm p} \frac{I}{I + I_{\rm d}}, \tag{1}$$

$$\hat{E}_{\rm sc} = \hat{E}_0 \frac{\hat{I}_\infty + \hat{I}_{\rm d}}{\hat{I} + \hat{I}_{\rm d}} + \hat{E}_{\rm p} \frac{\hat{I}_\infty - \hat{I}}{\hat{I} + \hat{I}_{\rm d}}, \tag{2}$$

where $E_0 = \pm g \hat{E}_{\rm p}$ for the configurations $\uparrow\uparrow$ and $\uparrow\downarrow$, respectively,

$$\hat{E}_0 = -\hat{\Gamma} \hat{E}_{\rm p},$$

$$g = \hat{\delta} \hat{I}_\infty \hat{W} \Phi / W,$$

$$\Phi = 1/[\delta I_{\rm d} + \hat{\delta}(\hat{I}_\infty + \hat{I}_{\rm d})],$$

$$\hat{\Gamma} = \hat{\delta} \hat{I}_\infty \Phi,$$

$$\delta = S\mu s_{\rm i}(N_{\rm D} - N_{\rm A})/(r_{\rm R} N_{\rm A} W),$$

$$E_{\rm p} = k_{\rm p} \gamma_{\rm R} N_{\rm A}/(e\mu),$$

$$\hat{\delta} = \hat{S}\hat{\mu}\hat{s}_{\rm i}(\hat{N}_{\rm D} - \hat{N}_{\rm A})/(\hat{r}_{\rm R}\hat{N}_{\rm A}\hat{W}).$$

Here $N_{\rm D}$ is the donor density, $N_{\rm A}$ is the acceptor density, $s_{\rm i}$ is the photoexcitation cross section, $\gamma_{\rm R}$ is the carrier recombination rate, μ and e are, respectively, the electron mobility and the charge, $k_{\rm p}$ is the photovoltaic constant, S is the surface of the electrodes of the crystals, W is the distance between the two electrodes, $I_{\rm d}$ is the so-called dark irradiance, $I = I(x, z)$ is the power density profile of the beam, and it attains asymptotically a constant value at $x \to \pm\infty$, that is, $I(x \to \pm\infty, z) = I_\infty$. These parameters with a symbol "$\hat{}$" for the crystal $\hat{P}$ have the same physical meaning as those without the symbol for the crystal P.

Although the expression of $E_{\rm sc}$ or $\hat{E}_{\rm sc}$ has the same form as that for a single biased PV-PR crystal,[6] $E_{\rm sc}$ and $\hat{E}_{\rm sc}$ are not independent of each other because they depend on the parameters of both crystals and the initial conditions of both solitons. In other words, the two fields are coupled each other by the parameters g and $\hat{\Gamma}$. Since g and $\hat{\Gamma}$ include the term of the peak input intensity of the dark soliton, namely $\hat{I}_\infty$, but do not include that of the bright soliton. Interestingly, varying the input intensity of the dark soliton can affect the bright one, but not vice versa. In this

paper, we pay our attention to how the variation of the input intensity of the dark soliton affects the self-deflection of the bright soliton. In order to simplify the problem, although the values of δ, W and $I_{\rm d}$ are in general different from those of $\hat{\delta}$, $\hat{W}$ and $\hat{I}_{\rm d}$, respectively, we here assume that $\delta = \hat{\delta}$, $W = \hat{W}$, and $I_{\rm d} = \hat{I}_{\rm d}$. In fact, $\delta = \hat{\delta}$ can be realized by adjusting the values of S and $\hat{S}$, and $I_{\rm d} = \hat{I}_{\rm d}$ can be realized by adjusting the temperature of the two crystals.[29] By use of these simplifications, parameter g has a simple expression as

$$g = \frac{\hat{\rho}}{2+\hat{\rho}}, \tag{3}$$

where $\hat{\rho} = \hat{I}_{\infty}/\hat{I}_{\rm d}$ is the peak input intensity of the dark soliton normalized to the dark irradiance.

$I = I(x,z)$ can be expressed in terms of the normalized envelope U in the form $I(x,z) = I_{\rm d}|U(x,z)|^2$, and U obeys the following dynamical evolution equation:

$$\mathrm{i}U_{\xi} + \frac{1}{2}U_{ss} - \beta\frac{U}{1+|U|^2} + \alpha\frac{|U|^2U}{1+|U|^2} = 0, \tag{4}$$

$$\mathrm{i}\hat{U}_{\hat{\xi}} + \frac{1}{2}\hat{U}_{\hat{s}\hat{s}} - \hat{\beta}(\hat{\rho}+1)\frac{\hat{U}}{1+|\hat{U}|^2} - \hat{\alpha}\frac{(\hat{\rho}-|\hat{U}|^2)\hat{U}}{1+|\hat{U}|^2} = 0, \tag{5}$$

where $\xi = z/(kx_0^2)$, $s = x/x_0$, $\beta = \sigma E_0$, $\alpha = \sigma E_{\rm p}$ and $\sigma = (k_0x_0)^2(n_{\rm e}^4r_{33}/2)$. Here x_0 is an arbitrary spatial width, $k = k_0n_{\rm e}$, $k_0 = 2\pi/\lambda_0$, and λ_0 is the free-space wavelength of the light wave employed, $n_{\rm e}$ is the unperturbed extraordinary index of refraction. Those parameters with a symbol "$\hat{\ }$" in Eq.(5) for the crystal $\hat{P}$ have the same expression and physical meaning as those without the symbol in Eq.(4) for the crystal P.

By expressing the beam envelope U in the usual fashion $U = r^{1/2}y(s)\exp(\mathrm{i}\nu\xi)$ for the bright soliton and $\hat{U} = \hat{\rho}^{1/2}\hat{y}(\hat{s})\exp(\mathrm{i}\hat{\nu}\hat{\xi})$ for the dark soliton, where the positive quantity r is the peak input intensity of the bright soliton normalized to the dark irradiance, i.e., $r = I_0/I_{\rm d} = I(0,0)/I_{\rm d}$; ν represents a nonlinear shift of the propagation constant, $y(s)$ is a normalized real function bounded between $0 \le y(s) \le 1$ and denotes the normalized field profile. The bright and dark soliton solutions can be derived from Eqs.(4) and (5) as follows:

$$(2G)^{1/2}s = \pm\int_{y(s)}^{1}\frac{r^{1/2}\mathrm{d}\tilde{y}}{[\ln(1+r\tilde{y}^2) - \tilde{y}^2\ln(1+r)]^{1/2}}, \tag{6}$$

$$(-2\hat{G})^{1/2}\hat{s} = \pm\int_{\hat{y}(\hat{s})}^{0}\frac{\mathrm{d}\tilde{y}}{\left[(\tilde{y}^2-1) - \dfrac{1+\hat{\rho}}{\hat{\rho}}\ln\left(\dfrac{1+\hat{\rho}\tilde{y}^2}{1+\hat{\rho}}\right)\right]^{1/2}}. \tag{7}$$

Here $\nu = -(G/r)\ln(1+r)$ and $\hat{\nu} = -\hat{G}$, where $G = \sigma(\pm g\hat{E}_{\rm p} + E_{\rm p})$ for the configurations $\uparrow\uparrow$ and $\uparrow\downarrow$, respectively, and $\hat{G} = \hat{\sigma}(1-\hat{I})\hat{E}_{\rm p}$ for both configurations $\uparrow\uparrow$ and $\uparrow\downarrow$.

The conditions necessary for a bright–dark soliton pair are $G > 0$ and $\hat{G} < 0$. From the two inequalities, one can obtain four approaches to obtain the bright–dark soliton pairs: (1) $E_{\rm p} > g|\hat{E}_{\rm p}|$, $\hat{E}_{\rm p} < 0$, $\uparrow\uparrow$; (2) $E_{\rm p} > 0$, $\hat{E}_{\rm p} < 0$, $\uparrow\downarrow$; (3) $E_{\rm p} < 0$, $\hat{E}_{\rm p} < 0$, $|E_{\rm p}| < g|\hat{E}_{\rm p}|$, $\uparrow\downarrow$; (4) $E_{\rm p} = 0$, $\hat{E}_{\rm p} < 0$, $\uparrow\downarrow$.

In order to describe the self-deflection of the bright soliton, we need to expand the above formulae about the bright soliton to include the terms of diffusion and higher-order space charge fields. When they are taken into account, the induced space charge field in the crystal P can be expressed as follows:[27]

$$E_{\rm sc} = E_{\rm sc0} + E_{\gamma} + E_{\gamma_1} + E_{\gamma_2} + E_{\gamma_3} + E_{\gamma_4}, \tag{8}$$

$$E_{\rm sc0} = E_0\frac{I_{\rm d}}{I+I_{\rm d}} - E_{\rm p}\frac{I}{I+I_{\rm d}}, \tag{9}$$

$$E_{\gamma} = -\frac{k_{\rm B}T}{e}\frac{1}{I+I_{\rm d}}\frac{\partial I}{\partial x}, \tag{10}$$

$$E_{\gamma_1} = -\frac{\varepsilon_0\varepsilon_{\rm r}}{eN_{\rm A}}E_0(E_0+E_{\rm p})\frac{I_{\rm d}^2}{(I+I_{\rm d})^3}\frac{\partial I}{\partial x}, \tag{11}$$

$$E_{\gamma_2} = -\frac{\varepsilon_0\varepsilon_{\rm r}}{eN_{\rm A}}E_{\rm p}(E_0+E_{\rm p})\frac{II_{\rm d}}{(I+I_{\rm d})^3}\frac{\partial I}{\partial x}, \tag{12}$$

where $k_{\rm B}$ is Boltzmann's constant, T is the absolute temperature, ε_0 is the free space permittivity, $\varepsilon_{\rm r}$ is the relative static dielectric constant. Because the higher-order fields E_{γ_3} and E_{γ_4} are much smaller than any of E_{γ}, E_{γ_1} and E_{γ_2}, we can ignore the effects of the two fields on the evolution and self-deflection of the solitons. Thus, the dynamical evolution equation about the normalized envelope U should be modified from Eq.(4) to the following form:[27]

$$\mathrm{i}U_{\xi} + \frac{1}{2}U_{ss} - \beta\frac{U}{1+|U|^2} + \alpha\frac{|U|^2U}{1+|U|^2} + \gamma\frac{(|U|^2)_sU}{1+|U|^2} + \gamma_1\frac{(|U|^2)_sU}{(1+|U|^2)^3} - \gamma_2\frac{|U|^2(|U|^2)_sU}{(1+|U|^2)^3} = 0. \tag{13}$$

Here $\alpha = \sigma E_{\rm p}$, $\beta = \sigma E_0$, $\gamma = \sigma\tau$, $\gamma_1 = \kappa_1(\alpha+\beta)$, $\gamma_2 = \kappa_2(\alpha+\beta)$, $\kappa_1 = \zeta E_0$, $\kappa_2 = \zeta E_{\rm p}$, $\sigma = (k_0x_0)^2(n_{\rm e}^4r_{33}/2)$, $\tau = k_{\rm B}T/(ex_0)$, $\zeta = \varepsilon_0\varepsilon_{\rm r}/(eN_{\rm A}x_0)$,

$U_\xi = \partial U/\partial\xi$, $U_{ss} = \partial^2 U/\partial s^2$. γ is the first-order diffusion term, γ_1 and γ_2 are the higher-order odd perturbation terms which will have odd effects (such as beam-deflection) as γ does. Since the even perturbation terms produce an even effect such as spatial broadening and play a negligible role on the process of the self-deflection,[26,27] they are omitted in our analysis in the paper.

The sign of E_p or $\hat{E}_p$ depends on the characteristics of the crystal and the polarization of the light. Since all the observations[7] indicate a negative perturbation in the index for $LiNbO_3$, E_p or $\hat{E}_p$ is always negative for $LiNbO_3$. Some photovoltaic materials (such as $BaTiO_3$), however, possess photovoltaic constants that change sign during polarization rotation.[30] This change results in an equivalent change of sign in the refractive-index perturbation and means that whether E_p or $\hat{E}_p$ is positive or negative depends on the polarization of the light.[7] Therefore, either a positive or a negative sign of E_p or $\hat{E}_p$ is possible for $BaTiO_3$.

The characteristics of the self-deflection of the bright soliton depend strongly on the signs of γ_1 and γ_2.[27] The sign of γ_1 is determined by the sign of $\hat{E}_p$ and the configuration of the crystal circuit, and the sign of γ_2 is determined by the sign of E_p. As described above, there are four approaches to obtain a bright–dark soliton pair in an unbiased series PR crystal circuit, and the signs of E_p and the configuration of the circuit are different for different approach; as a result, the signs of γ_1 and γ_2 are different for different approach and they are summarized in Table 1.

Table 1. The signs of γ_1 and γ_2 for different approaches.

Approaches	1	2	3	4
Conditions	$E_p > g\lvert\hat{E}_p\rvert$, $\hat{E}_p < 0, \uparrow\uparrow$	$E_p > 0$, $\hat{E}_p < 0, \uparrow\downarrow$	$E_p < 0, \hat{E}_p < 0$ $\lvert E_p\rvert < g\lvert\hat{E}_p\rvert, \uparrow\downarrow$	$E_p = 0$, $\hat{E}_p < 0, \uparrow\downarrow$
E_0	$E_0 = g\hat{E}_p < 0$	$E_0 = -g\hat{E}_p > 0$	$E_0 = -g\hat{E}_p > 0$	$E_0 = -g\hat{E}_p > 0$
Crystals	P : $BaTiO_3$ $\hat{P}$: $LiNbO_3$	P : $BaTiO_3$ $\hat{P}$: $LiNbO_3$	P : $BaTiO_3$ $\hat{P}$: $LiNbO_3$	P : SBN $\hat{P}$: $LiNbO_3$
Signs of γ_1 and γ_2	$\gamma_1 < 0, \gamma_2 > 0$	$\gamma_1 > 0, \gamma_2 > 0$	$\gamma_1 > 0, \gamma_2 < 0$	$\gamma_1 > 0, \gamma_2 = 0$
E_p/V· m^{-1}	2×10^6	1.5×10^6	-5×10^4	0
$\hat{E}_p$/V· m^{-1}	-1.2×10^6	-8×10^5	-5×10^5	-10^5
γ	0.204	0.204	0.204	0.56
σ/m·V^{-1}	3.16×10^{-4}	3.16×10^{-4}	3.16×10^{-4}	8.82×10^{-4}
ζ/m·V^{-1}	1.86×10^{-9}	1.86×10^{-9}	1.86×10^{-9}	3.04×10^{-8}
α	632	474	−15.8	0

In Eqs.(6) and (13), G, β, γ_1 and γ_2 depend on parameter g; as a result, they depend on $\hat{I}_\infty$ or $\hat{\rho} = \hat{I}_\infty/\hat{I}_d$. By use of Eq.(3), G, β, γ_1 and γ_2 can be expressed as

$$G = \sigma\left(E_p \pm \frac{\hat{\rho}}{2+\hat{\rho}}\hat{E}_p\right), \tag{14}$$

$$\beta = \pm\frac{\hat{\rho}}{2+\hat{\rho}}\sigma\hat{E}_p, \tag{15}$$

$$\gamma_1 = \pm\frac{\hat{\rho}}{2+\hat{\rho}}\zeta\sigma\hat{E}_p\left(E_p \pm \frac{\hat{\rho}}{2+\hat{\rho}}\hat{E}_p\right), \tag{16}$$

$$\gamma_2 = \zeta\sigma E_p\left(E_p \pm \frac{\hat{\rho}}{2+\hat{\rho}}\hat{E}_p\right), \tag{17}$$

where the signs + and − correspond to the configurations $\uparrow\uparrow$ and $\uparrow\downarrow$, respectively.

3. Numerical results

In this paper, we always take λ_0=0.5 μm, x_0=40 μm and T=300 K. Because $\hat{E}_p$ is always negative for every approach, we choose $LiNbO_3$ as the crystal $\hat{P}$. For approaches 1 to 3, we choose $BaTiO_3$ as the crystal P with the following parameter values: n_e=2.365, $\gamma_{33} = 80 \times 10^{-12}$ m/V, $N_A = 10^{17}$ cm^{-3}, ε_r=135. For approach 4, we choose SBN (strontium barium niobate) as the crystal P with the following parameter values: $\gamma_{33} = 237 \times 10^{-12}$ m/V, n_e=2.33, $N_A = 4 \times 10^{16}$ cm^{-3}, ε_r=880, E_p=0. The chosen values of E_p and $\hat{E}_p$ as well as the corresponding calculated values of α, γ, σ and ζ are listed in Table 1.

Dynamical evolutions of the bright and dark solitons in a bright–dark pair were investigated in Ref.[22]. In this paper, we are only concerned with how the variation of the input intensity of the dark soliton affects the self-deflection of the bright soliton; as a result, we only investigate the dynamical self-deflection evolution of the bright soliton when the diffusion term and the higher-order space charge fields are taken into account. We give one example for each approach. If a bright soliton is incident upon the crystal P, its dynamical evolution can be obtained by numerically solving Eq.(13) when the values of r, $\hat{\rho}$, α, β, γ, γ_1 and γ_2 are given. If we assume r=10 and $\hat{\rho}$=10, and take the values of α and γ from Table 1, as well as the calculated values of β, γ_1 and γ_2 from Eqs.(15)–(17) with the values of σ, ζ, $E_{\rm p}$ and $\hat{E}_{\rm p}$ from Table 1, we have the following results: (1) approach 1, α=632, $\beta = -316$, γ=0.204, $\gamma_1 = -0.5895$, and γ_2=1.179; (2) approach 2, α=474, β=211, γ=0.204, γ_1=0.851, and γ_2=1.92; (3) approach 3, $\alpha = -15.8$, β=131, γ=0.204, γ_1=0.09, and $\gamma_2 = -0.011$; and (4) approach 4, α=0, β=73.5, γ=0.57, γ_1=0.186, and γ_2=0. The input bright soliton for each approach is $U_j = \sqrt{10}y_j(s)$ (j=1,2,3,4), in which $y_j(s)$ can be obtained from Eq.(6) with r=10 and $G = \alpha + \beta$, that is, (1) G=316; (2) G=685; (3) G=115; and (4) G=73.5. The dynamical evolution of U_j (j=1,2,3,4) is shown in Fig.2. The corresponding spatial shift of the beam centre (denoted by Δs) of U_j (j=1,2,3,4) as a function of ξ is shown in Fig.3 (solid curves a–d). From Figs 2 and 3 we can see that the bright soliton experiences approximately adiabatic self-deflection and moves approximately on a parabolic trajectory for each approach; however, sometimes it bends left and sometimes right (bending left or right means the deflection of the soliton bending in the same direction as the crystal's c-axis or in an opposite direction). Like a bright solitons in a single biased PV-PR crystal, bending right or left depends on the sign and strength of the two photovoltaic fields and the incident optical intensity of the bright soliton.[27] For approach 4, the crystal P is non-PV-PR; therefore, the bright soliton is a screening soliton[4] and then can only bend right.[25–27] For approaches 1 and 2, because the crystal P is PV-PR and $E_{\rm p} > 0$, the bright soliton is a screening-photorefractive soliton[6] and then can bend both right and left, however, whether it bends right or left depends on the incident intensity of the bright soliton.[27] Furthermore, for approach 3, although the crystal P is PV-PR and then the bright soliton is a screening-photorefractive soliton, the bright soliton can only bend right because $E_{\rm p} < 0$.[27]

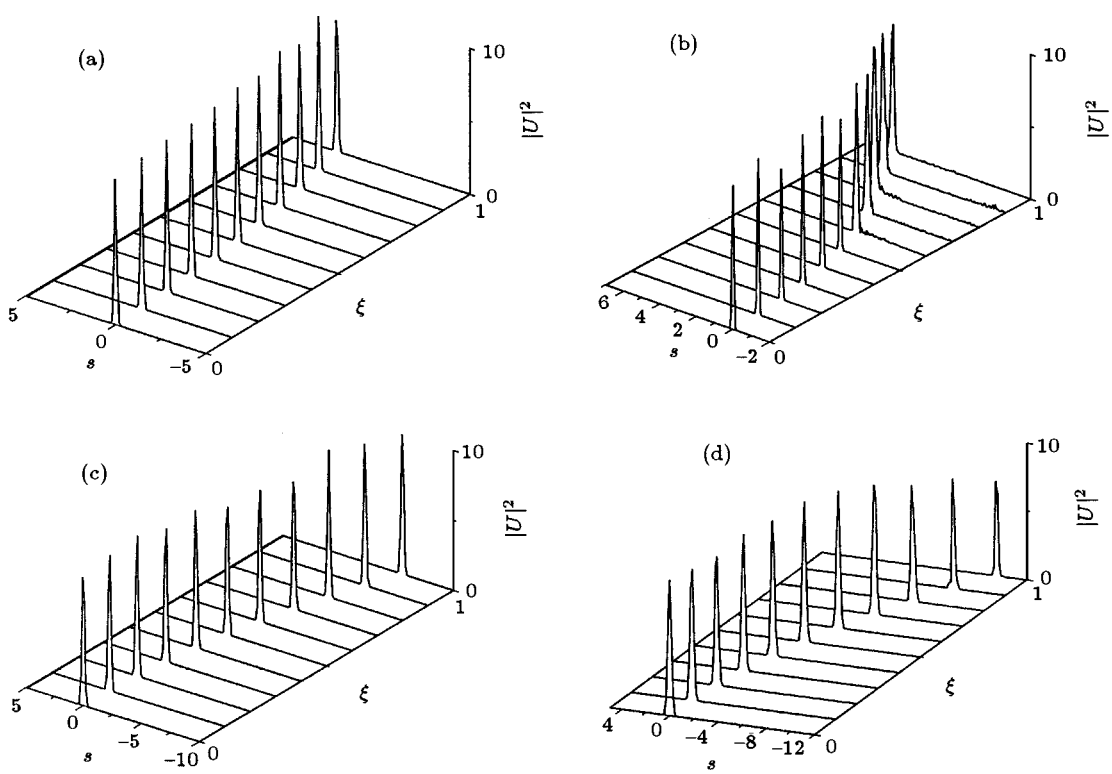


Fig.2. The dynamical evolution of a bright soliton in crystal P for each approach. (a)–(d) correspond to approaches 1 to 4, respectively.

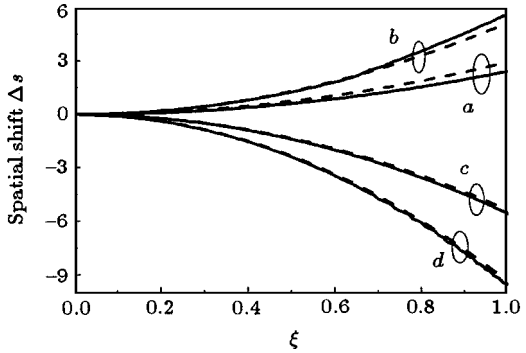


Fig.3. The spatial shifts of the beam centre of a bright soliton as a function of ξ in crystal P for each approach corresponding to the results shown in Fig.2. The solid curves are obtained using the numerical method and the dashed curves are obtained using the perturbative procedure.

We then investigate the effects of the input intensity of the dark soliton on the ξ dependence of Δs. To do so, we take four values of $\hat{\rho}$ as 1,10,100, and 1000 for each approach. The corresponding values of G, α, β, γ, γ_1, and γ_2 are listed in Table 2 for all the four approaches. Thus we have four bright–dark soliton pairs in which the four bright solitons have the same value of the normalized peak input intensity, i.e., r=10; whereas the four dark solitons have the value of $\hat{\rho}$ as 1,10,100, and 1000, respectively. Figure 4 gives the ξ dependence of Δs for different values of $\hat{\rho}$ for all the four approaches. Each curve in Fig.4, its corresponding parameter values being listed in Table 2, is obtained by numerically solving Eq.(13) with a bright solitary state as the input beam profile that is obtained from Eq.(6) with a set of values of r and G. Here r is always set at r=10, but G takes different value for different case, as listed in Table 2. These results show that, for a given value of ξ, such as ξ=1, Δs is a nonlinear function of $\hat{\rho}$.

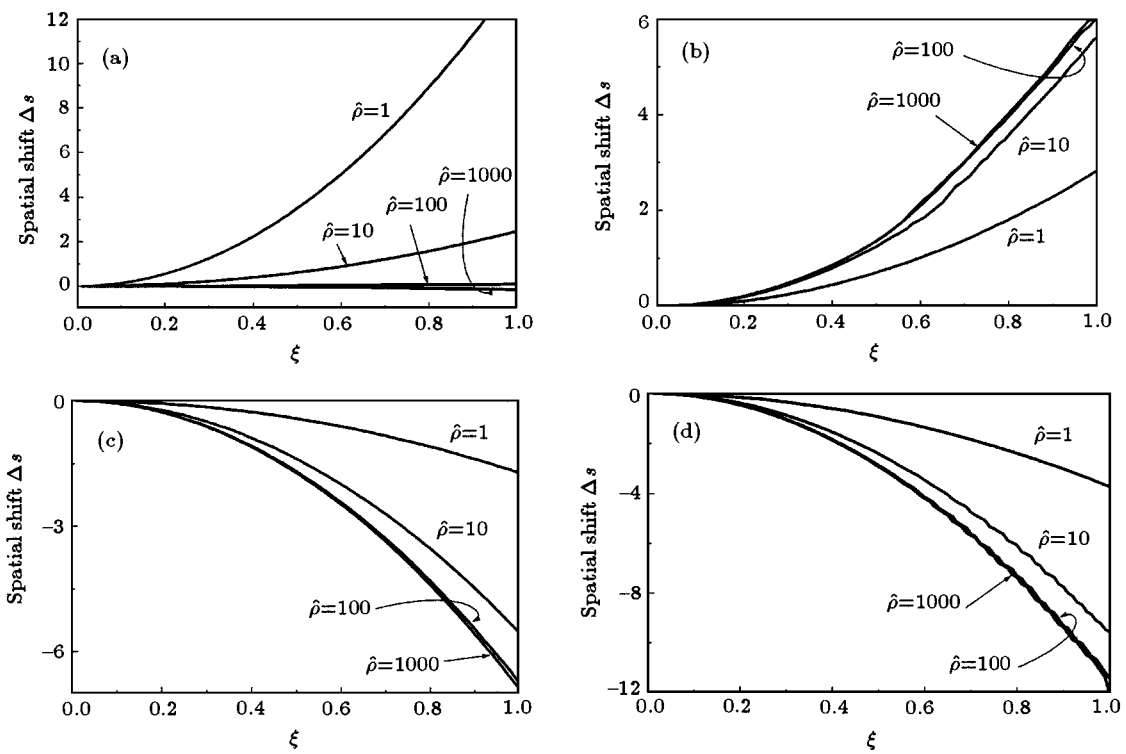


Fig.4. The spatial shifts, Δs, of the beam centres of the four bright solitons in crystal P. (a)–(d) correspond to approaches 1 to 4, respectively.

Table 2. The parameter values used for Fig.4.

Approach 1							Approach 2						
$\hat{\rho}$	G	α	β	γ	γ_1	γ_2	$\hat{\rho}$	G	α	β	γ	γ_1	γ_2
1	506	632	–126	0.204	–0.377	1.886	1	558	474	84	0.204	0.278	1.56
10	316	632	–316	0.204	–0.589	1.18	10	685	474	211	0.204	0.85	1.92
100	260	632	–372	0.204	–0.57	0.971	100	722	474	248	0.204	1.056	2.02
1000	253	632	–379	0.204	–0.566	0.946	1000	726	474	252	0.204	1.081	2.03

Table 2. (*Continued*)

Approach 3							Approach 4						
$\hat{\rho}$	G	α	β	γ	γ_1	γ_2	$\hat{\rho}$	G	α	β	γ	γ_1	γ_2
1	37.9	–15.8	52.7	0.204	0.0115	–0.0034	1	29.4	0	29.4	0.57	0.03	0
10	115.2	–15.8	131	0.204	0.09	–0.011	10	73.5	0	73.5	0.57	0.186	0
100	139.2	–15.8	155	0.204	0.127	–0.013	100	86.5	0	86.5	0.57	0.258	0
1000	142	–15.8	157.8	0.204	0.132	–0.0132	1000	88.1	0	88.1	0.57	0.267	0

4. Perturbative procedure

Although from Fig.4 we can see that for a given value of ξ, Δs is an increasing or decreasing function of $\hat{\rho}$, it is difficult to obtain a comprehensive image by use of the numerical method. Therefore, we will use a perturbative procedure to derive an approximate analytical expression for Δs varying with $\hat{\rho}$, from which we can obtain more comprehensive information than that from the numerical results. The perturbative procedures were previously employed within the context of nonlinear fibre optics[31,32] and have been used to investigate the self-deflection process of bright screening solitons with[26] and without[25] higher-order terms, as well as the bright screening-photovoltaic solitons with[27] and without[6] higher-order terms.

The solution of Eq.(13) is obtained as the following ansatz:[6,25–27]

$$U = r^{1/2} y[s + u(\xi)] \times \exp\{\mathrm{i}[\nu\xi + \omega(\xi)(s + u(\xi)) + \sigma(\xi)]\}, \quad (18)$$

where $U = r^{1/2} y(s)\exp(\mathrm{i}\nu\xi)$ is the steady-state bright soliton of Eq.(13) with γ=0 and γ_i=0 (i=1,2). In Eq.(18), $u(\xi)$ represents a shift of the position of the beam centre, $\omega(\xi)$ is associated with the angle between the central wavevector of this beam and the propagation axis ξ, and $\sigma(\xi)$ is a phase factor which is allowed to vary during propagation. The equations of motion of these real variables can be obtained by substituting Eq.(18) into the two complex conservation laws of Eq.(13) and have the following forms:[27]

$$\mathrm{d}u(\xi)/\mathrm{d}\xi = -\omega(\xi),$$

$$\mathrm{d}\sigma(\xi)/\mathrm{d}\xi = \omega^2(\xi)/2,$$

$$\mathrm{d}\omega(\xi)/\mathrm{d}\xi = 4(\beta + \alpha)[\gamma K(r) + \gamma_1 K_1(r) - \gamma_2 K_2(r)],$$

where the dimensionless functions $K(r)$, $K_1(r)$ and $K_2(r)$ are given by

$$K(r) = \int_{-\infty}^{+\infty} \mathrm{d}s \frac{2y^2(s)}{1 + ry^2(s)} \times \{y^2(s)\ln(1 + r) - \ln[1 + ry^2(s)]\} \left(\int_{-\infty}^{+\infty} \mathrm{d}s y^2(s) \right)^{-1}, \quad (19)$$

$$K_1(r) = \int_{-\infty}^{+\infty} \mathrm{d}s \frac{2y^2(s)}{[1 + ry^2(s)]^3} \times \{y^2(s)\ln(1 + r) - \ln[1 + ry^2(s)]\} \left(\int_{-\infty}^{+\infty} \mathrm{d}s y^2(s) \right)^{-1}, \quad (20)$$

$$K_2(r) = \int_{-\infty}^{+\infty} \mathrm{d}s \frac{2ry^4(s)}{[1 + ry^2(s)]^3} \times \{y^2(s)\ln(1 + r) - \ln[1 + ry^2(s)]\} \left(\int_{-\infty}^{+\infty} \mathrm{d}s y^2(s) \right)^{-1}. \quad (21)$$

The values of $K(r)$, $K_1(r)$ and $K_2(r)$ are always negative and tend to be zero when r tends to be zero or infinity.[27] Although $K(r)$, $K_1(r)$ and $K_2(r)$ mainly rely on r and are insensitive to $G = \alpha + \beta$ (hence to $\hat{\rho}$),[27] it is necessary to depict the behaviour as a function of $\hat{\rho}$ for $K(r)$, $K_1(r)$ and $K_2(r)$ as shown in Fig.5, for the main aim of this paper is to investigate the $\hat{\rho}$ dependence of Δs at ξ=1. The results show that, compared with the wide variation range of $\hat{\rho}$, i.e., $\hat{\rho} \in [0.01, 1000]$, the variation in the values of $K(r)$, $K_1(r)$ or $K_2(r)$ is quite small. For approach 3, the range of $\hat{\rho}$ is limited, i.e., it cannot be taken too small or else the conditions necessary for a bright–dark soliton pair will not be satisfied. In other words, the value of $\hat{\rho}$ must be taken large enough so that the value of g can ensure $g|\hat{E}_\mathrm{p}| > |E_\mathrm{p}|$.

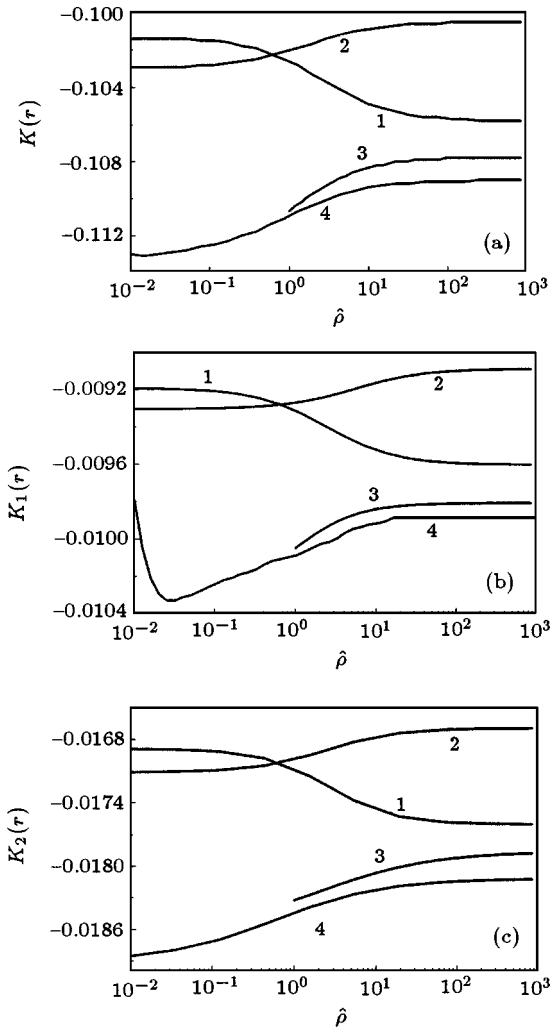


Fig.5. The dependence of $K(r)$, $K_1(r)$ and $K_2(r)$ on $\hat{\rho}$ for all the four approaches with r=10 and the values of $E_{\rm p}$, $\hat{E}_{\rm p}$, and σ being taken from Table 1. (a) $K(r)$-$\hat{\rho}$; (b) $K_1(r)$-$\hat{\rho}$; and (c) $K_2(r)$-$\hat{\rho}$.

Because the spatial shifts $\Delta s(\xi) = -u(\xi)$ and $u(\xi)$ can then be directly integrated,[27] we can obtain

$$\Delta s(\xi) = 2G[\gamma K(r) + \gamma_1 K_1(r) - \gamma_2 K_2(r)]\xi^2. \quad (22)$$

By use of this equation, we recalculate the ξ dependence of Δs with the parameter values the same as those solid curves shown in Fig.3, from which we can see that the results obtained from the analytical method are in good agreement with those obtained from the numerical methods.

We assume that the normalized length of crystal P is ξ=1, thus $\Delta s_0 \equiv \Delta s(\xi = 1)$ denotes the spatial shift of the beam centre of the bright soliton at the output surface of crystal P. In fact, Δs_0 denotes the amount of deflection when a bright solitary beam is incident on the crystal, and an expression for Δs_0 as a function of $\hat{\rho}$ can then be derived from Eqs.(14)–(17) and (22) as follows:

$$\begin{aligned}\Delta s_0 =& 2\sigma\left(E_{\rm p} \pm \frac{\hat{\rho}}{2+\hat{\rho}}\hat{E}_{\rm p}\right) \\ &\times \left[\gamma K(r) \pm \frac{\hat{\rho}}{2+\hat{\rho}}\zeta\sigma\hat{E}_{\rm p}\left(E_{\rm p} \pm \frac{\hat{\rho}}{2+\hat{\rho}}\hat{E}_{\rm p}\right)K_1(r)\right. \\ &\left. - \zeta\sigma E_{\rm p}\left(E_{\rm p} \pm \frac{\hat{\rho}}{2+\hat{\rho}}\hat{E}_{\rm p}\right)K_2(r)\right], \quad (23)\end{aligned}$$

where the signs + and − correspond to the configurations ↑↑ and ↑↓, respectively. Obviously, Δs_0 is a nonlinear function of $\hat{\rho}$. Although all of the values of $K(r)$, $K_1(r)$, $K_2(r)$ are negative, either a positive or a negative sign of Δs_0 is possible because either a positive or a negative sign of $E_{\rm p}$ is possible. This fact means that when a bright solitary beam is incident upon crystal P with its propagation direction normal to the direction of the c-axis of the crystal, the output beam can bend both in the same direction as and in the direction opposite to the c-axis, and which direction it will bend to depends on the values of r and $\hat{\rho}$, the sign and strength of $E_{\rm p}$ and $\hat{E}_{\rm p}$, as well as the configurations ↑↑ and ↑↓.

Figure 6 gives the $\hat{\rho}$ dependence of Δs_0 calculated from Eq.(23) as well as Eqs.(19)–(21) under different values of r, i.e., r=1,10, and 100 for all the four approaches. The results in Fig.6 show that Δs_0 is a nonlinear function of $\hat{\rho}$. When $\hat{\rho}$ increases from its initial to the final value, for approach 1 with r=100 and approach 2 with r=10, the bright solitary beam scans toward the same direction as the crystal's c-axis, while in the other cases toward the direction opposite to the crystal's c-axis. For all the four approaches, when $\hat{\rho}$ is weak or strong enough, Δs_0 is kept unchanged with increasing $\hat{\rho}$, whereas Δs_0 increases or decreases monotonically with $\hat{\rho}$ in the middle range of $\hat{\rho}$. If we define $\delta s = |\Delta s_0(\hat{\rho} \to 0) - \Delta s_0(\hat{\rho} \to \infty)|$ as the deflection range of the bright solitary beam, from Fig.6 we can see that δs depends strongly on r in each approach. Taking approach 1 as an example, from Fig.6 (a) we can see that, $\delta s(r = 10) \gg \delta s(r = 100)$. These results indicate that under some conditions varying $\hat{\rho}$ can adjust the value of Δs_0 in a wide range, but under the other conditions only in a narrow range. Whether the deflection range is wide or narrow depends on the value of r, the sign and strength of $E_{\rm p}$ and $\hat{E}_{\rm p}$ as well as the configurations ↑↑ and ↑↓. For a given approach, the value of r is a crucial factor. Taking approach 2 as an example, if we want a large deflection range, we should take r=1 whereas we should take r=100 if we want a small one.

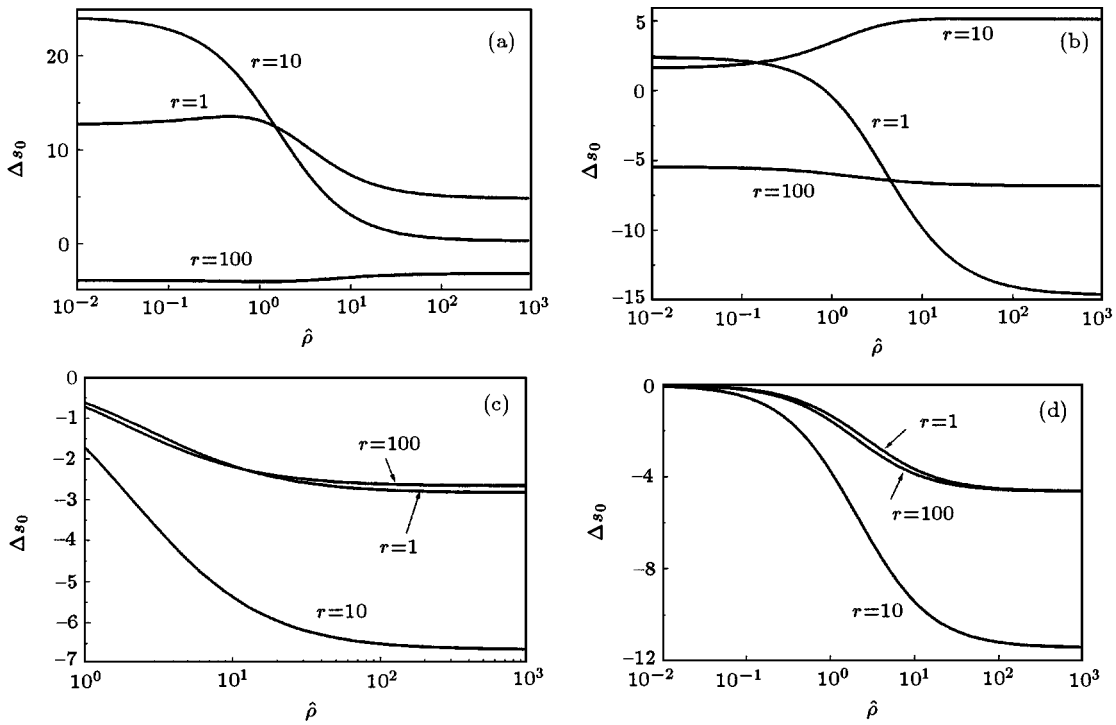


Fig.6. The dependence of Δs_0 on $\hat{\rho}$ with r=1,10, and 100 for all the four approaches. The values of $E_{\rm p}$, $\hat{E}_{\rm p}$, ζ and σ are taken from Table 1. Here (a)–(d) correspond to approaches 1 to 4, respectively.

Figure 7 gives the r dependence of δs for all the four approaches by solving Eq.(23) and Eqs.(19)–(21), as well as $\delta s = |\Delta s_0(\hat{\rho}=\hat{\rho}_0) - \Delta s_0(\hat{\rho}=1000)|$ in which $\hat{\rho}_0$=0.01 for approaches 1, 2 and 4, and $\hat{\rho}_0$=1 for approach 3. From Fig.7 we can see that δs will tend to zero when r is small or big enough for all the four approaches; however, in the middle range, the different approach possesses different characteristic. For approaches 3 and 4, δs has only one peak point. When r=4.92 and 7.1, δs reaches its maximum value 5.13 and 11.53, respectively. For approaches 1 and 2, δs has several peak and valley points. For approach 1, when r=0.23, 4.92 and 300, δs reaches its peak values 0.65, 29.9 and 1.71, respectively; when r=0.38 and 76, δs reaches its valley values 0.15 and 0.31, respectively. For approach 2, when r=1.15, 12.2 and 158, δs reaches its peak values 16.97, 3.6 and 1.47, respectively; when r=5 and 44, δs reaches its valley values 0.48 and 0.02, respectively. Such a character of δs varying with r permits us to select the self-deflection of the bright soliton to be sensitive or insensitive to the input intensity of the dark soliton by selecting the value of the input intensity of the bright soliton. Taking approach 2 as an example, if we want to have a large deflection range, we should take r near 1.15, whereas we should take r near 5 or 44 if we want to have a small range. In fact, when r=44, δs comes near zero, indicating that the deflection amount of the bright soliton barely varies with the input intensity of the dark soliton.

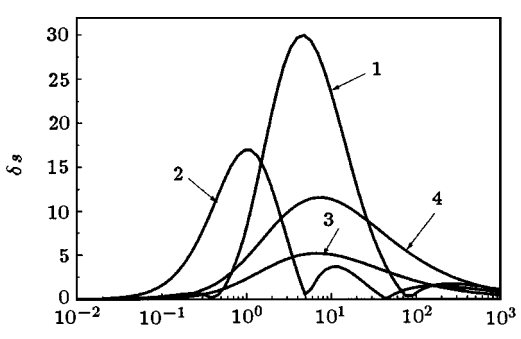


Fig.7. The r dependence of δs. The values of $E_{\rm p}$, $\hat{E}_{\rm p}$, ζ and σ are taken from Table 1. Curves 1–4 correspond to approaches 1 to 4, respectively.

From Eqs.(22) and (23) we can see that coactions of $K(r)$, $K_1(r)$ and $K_2(r)$ cause δs to have several peak and valley points for approaches 1 and 2, although there is only one peak point in the curves of $|K(r)|$, $|K_1(r)|$ and $|K_2(r)|$ versus r.[27] However, for approaches 3 and 4, from Table 1 we can see that, $E_{\rm p}$ and $\hat{E}_{\rm p}$ are not strong enough; as a result, the absolute values of the higher-order odd perturbation terms (i.e., γ_1 and γ_2) will be smaller or much smaller than that of the first-order diffusion term (i.e., γ). Furthermore, the absolute value of $K(r)$ is much larger than

that of $K_1(r)$ or $K_2(r)$.[27] Thereby, the r dependence of δs will be mainly determined by $\gamma K(r)$, other than by the coactions of $\gamma K(r)$, $\gamma_1 K_1(r)$ and $\gamma_2 K_2(r)$ if $E_{\rm p}$ and $\hat{E}_{\rm p}$ are not strong enough. Hence, δs has only one peak point for approaches 3 and 4. Obviously, the higher-order space charge fields play an important role in the r dependence of δs when $E_{\rm p}$ and $\hat{E}_{\rm p}$ are strong enough.

5. Conclusion

In conclusion, we have investigated by both numerical and perturbation methods the self-deflection of the bright soliton as a function of the input intensity of the dark soliton in a separate bright–dark soliton pair supported by an unbiased series PR crystal circuit when the effects of higher-order space charge fields are taken into account. Four possible approaches to realize a bright–dark soliton pair in the crystal circuit are considered. Numerical and analytical results show that varying the input intensity of the dark soliton ($\hat{\rho}$) can effectively adjust the deflection amount and direction of the bright soliton. The deflection amount (Δs_0), defined as the value of the spatial shift of the bright solitary beam centre at the output surface of the crystal, is a monotonic and nonlinear function of $\hat{\rho}$. When $\hat{\rho}$ is weak or strong enough, Δs_0 is, in fact, unchanged with $\hat{\rho}$, whereas Δs_0 increases or decreases monotonically with $\hat{\rho}$ in a middle range of $\hat{\rho}$. The corresponding variation range (δs) depends strongly on the value of the input intensity of the bright solitary beam (r). There are some peak and valley values in the curve of δs varying with r for two approaches, whereas there is only one peak point for the other two approaches. When $\hat{\rho}$ increases, the bright solitary beam can scan toward both the same direction as and the direction opposite to the crystal's c-axis. Whether the direction in the same or in the opposite direction will depend on the value of r, the parameter values and configuration of the crystal circuit. The different approach possesses different character in the self-deflection of the bright soliton as a function of the input intensity of the dark soliton. A novel optically controlled beam deflector or scanner can be possibly made up based on the principle presented in this paper. Such a passive device possesses the following character, namely, to use different values of the input intensity of the controlled beam can obtain the different scanning direction and range.

References

[1] Zakharov V E and Shabat A B 1972 *Phys. JETP* **34** 62
Zakharov V E and Shabat A B 1973 *Phys. JETP* **37** 823
[2] Trillo S and Torruellas W 2001 *Spatial Solitons* (Berlin: Springer)
[3] Segev M, Crosignani B, Yariv A and Fischer B 1992 *Phys. Rev. Lett.* **68** 923
[4] Christodoulides D N and Carvalho M I 1995 *J. Opt. Soc. Am.* B **12** 1628
[5] Segev M, Valley G C, Bashaw M C, Taya M and Fejer M M 1997 *J. Opt. Soc. Am.* B **14** 1772
[6] Liu J S and Lu K Q 1999 *J. Opt. Soc. Am.* B **16** 550
[7] Valley G C, Segev M, Crosignani B, Yariv A and Bashaw M C 1994 *Phys. Rev.* A **50** R4457
[8] Segev M, Valley G C, Crosignani B, Diporto P and Yariv A 1994 *Phys. Rev. Lett.* **73** 3211
[9] Duree G C, John Jr and Shultz L 1993 *Phys. Rev. Lett.* **71** 533
[10] Liu J S 2001 *Chin. Phys.* **10** 1037
[11] Shih M F, Segev M, Valley G C, Salamo G, Crosignani B and Porto P D 1995 *Elect. Lett.* **31** 826
[12] Taya M, Bashaw M, Fejer M M, Segev M and Vally G C 1995 *Phys. Rev.* A **52** 3095
[13] Christodoulides D N, Singh S R and Carvalho M I 1996 *Appl. Phys. Lett.* **68** 1763
[14] Shih M and Segev M 1996 *Opt. Lett.* **21** 1538
[15] Chen Z, Segev M, Coskun T H, Christodoulides D N and Kivshar Y S 1997 *J. Opt. Soc. Am.* B **21** 3066
[16] Krolikowski W and Holmstrom S A 1997 *Opt. Lett.* **22** 369
[17] Mamaev A V, Saffman M and Zozulya A A 1998 *J. Opt. Soc. Am.* B **15** 2097
[18] Chen Z, Acks M, Ostrovskaya E A and Kivshar Y S 2000 *Opt. Lett.* **25** 417
[19] Hou C F, Zhou Z X, Sun X D and Yuan B H 2001 *Optik* **112** 17
[20] Liu J S and Hao Z H 2002 *Phys. Rev.* E **65** 066601
[21] Liu J S 2002 *Phys. Lett.* A **300** 213
[22] Liu J S and Hao Z H 2003 *Phys. Lett.* A **309** 44
[23] Shih M F, Leach P, Segev M, Garret M H, Gsalamo G and Valley G C 1995 *Opt. Lett.* **21** 324
[24] Petter J, Weilbau C, Denz C, Stepken A and Kaiser F 1999 *Opt. Comm.* **170** 291
[25] Carvalho M I, Singh S R and Christodoulides D N 1995 *Opt. Comm.* **120** 311
[26] Singh S R, Carvalho M I and Christodoulides D N 1996 *Opt. Comm.* **130** 288
[27] Liu J S and Hao Z H 2002 *J. Opt. Soc. Am.* B **19** 513
[28] Liu J S and Hao Z H 2001 *J. M. Opt.* **48** 1803
[29] Liu J S and Hao Z H 2001 *Phys. Lett.* A **285** 377
[30] Sturman B I and Fridkin V M 1992 *The Photovoltaic and Photorefractive Effect in Non-centrosymmetric Materials* (Philadelphia: Gordon and Breach)
[31] Kodama Y and Hasegawa A 1987 *IEEE J. Quan. Elec.* **23** 510
[32] Blow K J, Doran N J and Wood D 1988 *J. Opt. Soc. Am.* B **5** 1301